SUPPORTING INFORMATION

Chemically Transformed Monolayers on Acene Thin Films for Improved Metal/Organic Interfaces

Feifei Li,‡[a] Jonathan P. Hopwood,‡[a] Melissa M. Galey, [b] Laura M. Sanchez[b] and Jacob W. Ciszek*[a]

[1]Department of Chemistry and Biochemistry, Loyola University Chicago, Chicago, IL, USA, Email: jciszek@luc.edu
[2]Department of Pharmaceutical Science, University of Illinois at Chicago, Chicago, IL, USA
‡ These authors contributed equally to this work.

Table of Contents

General Experimental Methods:

Maleic Anhydride Terminated Tetracene Thin Films

Precursor films (maleic anhydride terminated tetracene) were prepared following previously reported procedures.[1] Briefly, 50 nm of sublimed grade tetracene, (>99.99%) was deposited onto freshly prepared gold slides at a rate of 1 Å/s using a home built deposition chamber at a base pressure < 3×10^{-5} Torr. Thin films were terminated with maleic anhydride by placing them in a Schlenk tube with 10 mg of source material, under nitrogen, for 48 h at 40 ºC, and afterwards non-chemisorbed materials were removed via vacuum.

Chemical Transformations of Thin Films

Maleic anhydride terminated thin-films were placed in a drying chamber with a small vial containing the source material (~0.5 g of water or *n*-butylamine, 0.010 g of cysteamine). The drying chamber was then evacuated and filled with nitrogen three times before it was sealed. The chamber was then placed in a furnace at the appropriate temperatures (water: 70 °C, *n*-butylamine: 40 °C, cysteamine: 40 °C). Once the reaction was completed, the chamber was evacuated to less than 10^{-2} Torr and the base was cooled to -78 ºC to remove any vapors and physisorbed material from the film (1 h). Secondary reactions of tetracene thin-films were examined using a Bruker Optics Tensor 37 FT-IR with a polarization modulation accessory (PMA 50) and MCT detector.

Mass Spectrometry Analysis

Mass spectrometry samples were reacted under similar conditions described above, with the primary difference being the larger substrate size (75×25 mm vs 30×10). After secondary reaction and IR analysis, samples were then coated with α-cyano-4-hydroxycinnamic acid (CHCA) matrix via an HTX TM-sprayer from a stock solution of 5 mg/mL CHCA in 9:1 acetonitrile:water at 70 ºC with a flow rate of 0.100 mL/min. Coated samples were then examined with a Bruker Autoflex Speed MALDI-TOF equipped with a smartbeam-II laser (355 nm) in positive reflectron mode (laser power: 40%; laser spot size: large; detector gain: 8×). Prior to data acquisition, the instrument was calibrated to a peptide standard (Bruker Daltonics GmbH).

X-ray Photoelectron Spectroscopy Analysis

A Kratos AXIS-165 XPS was used to analyze cysteamine secondary reactions of precursor thin films. Photoelectrons were produced from a monochromatic Al X-ray source at an incident angle of 45° with a spot size of 200 μm and a chamber pressure of 3×10^{-10} Torr. All acquired spectra were baselined and deconvoluted using XPSPEAK 4.1 software. A Tougaard type background subtraction was used for O1s, N1s, and S2p signals while a Shirley type background subtraction was used for C1s signals. All samples were referenced to the C1s line at 284.6 eV.[2]

Bending Tests

All preparations were identical except for the thickness of the starting tetracene thin film (150 nm) and that films were deposited onto a gold coated PET substrate (rather than a gold slide). One set of samples was set aside without reaction. The remaining samples were reacted to form the maleic anhydride precursor followed by secondary reaction with cysteamine. Thermally deposited silver electrodes (80 nm) were evaporated onto the samples at a rate of 1 Å/s using a Kurt J. Lesker NANO 38 evaporator at a base pressure of $<1 \times 10^{-6}$ Torr utilizing a Ossila shadow mask to define the electrode features (mask E291). Each set of devices was located on an area of the PET that was approximately 3 cm^2 in area. The bending test was performed following ASTM standard (D790)[3] by fixing the squares at both ends of the silver electrode, pushing both sides in form of a U-shape from 1-100 times. The bending diameter was approximately 5 mm. Each of the five silver electrodes generated (per sample) were examined under SEM and accompanying images are representative. The films were imaged using a Hitachi SU3500 scanning electron microscope at up to 18000× magnification with accelerating voltage of 1.75 kV. The film was loaded on a 45° stub holder and was then manual titled 25°, in total 70° for all the SEM images.

Synthetic Methods:

All reactions were run under a nitrogen atmosphere and solvents were purged unless otherwise stated. All column chromatography separations were performed on silica gel 60 (40-63 μm from BDH). Thin layer chromatography was carried out on silica gel (F_{254}) with glass support. All NMR spectra were taken on a Varian 500 MHz spectrometer. ^1H and ^{13}C chemical shifts (δ) in $CDCl_3$ were referenced to tetramethylsilane. ^1H and ^{13}C chemical shifts (δ) in DMSO-d_6 were referenced to its residual solvent signal (2.50 and 39.51 respectively).[4] IR spectra were acquired on a Shimadzu IRAffinity-1S FTIR with a Pike Technologies MIRacle single reflection horizontal ATR accessory. 5,12-Dihydro-5,12-ethano-napthacene-13,14-dicarboxylic acid anhydride (maleic anhydride adduct, **1**) was synthesized using a previous procedure.[5]

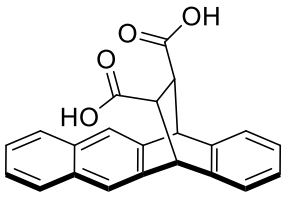

5,12-Dihydro-5,12-ethano-napthacene-13,14-dicarboxylic acid (2): 5,12-Dihydro-5,12-ethano-napthacene-13,14-dicarboxylic acid anhydride (0.0329 g, 0.101 mmol) was added to a sealed tube which was evacuated and filled with nitrogen three times. Water (0.5 mL, 27.7 mmol) and THF (1 mL) were added to the tube which was sealed and placed in an oil bath at 70 °C. After 43 h, the tube was removed from the oil bath and cooled to room temperature. The

solvent was then removed and CH_2Cl_2 added to form a white precipitate that was collected via vacuum filtration. This yielded the desired diacid (**2**) as white powder (0.0129 g, 0.0374 mmol) in 37 % yield as a single isomer. ^{1}H NMR (500 MHz, DMSO-d_6) δ 12.04 (s, 2H), 7.84-7.80 (m, 4H), 7.44 (dd, J = 6.2, 3.3 Hz, 2H), 7.30 (dd, J = 5.3, 3.3 Hz, 2H), 7.07 (dd, J = 5.4, 3.2 Hz, 2H), 4.69 (s, 2H), 3.17 (s, 2H). ^{13}C NMR (125 MHz, DMSO-d_6) δ 172.4, 140.9, 140.5, 131.6, 127.3, 125.41, 125.36, 124.9, 121.1, 47.3, 46.3. IR (cm^{-1}) 1713, 1501, 1479, 1414, 1315, 1227, 1207, 889, 748, 673.

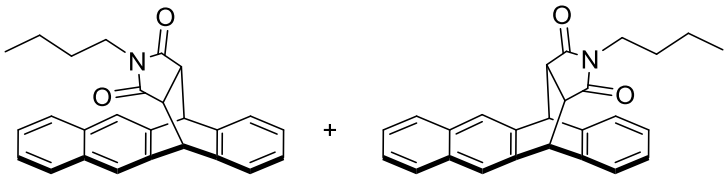

5,12-Dihydro-5,12-ethano-napthacene-15-*N*-butylpyrrolidine-14,16-dione (3a): Tetracene (0.0448 g, 0.196 mmol) and *n*-butylmaleimide (0.0399 g, 0.260 mmol) were added to a tube which was evacuated and filled with nitrogen three times. Toluene (2 mL) was then added to the tube, which was then sealed and placed in an oil bath at 120 °C. After 48 h, the reaction was cooled to room temperature and the solvent was removed. The crude product was purified via column chromatography (1:4 EtOAc: hexanes, R_f: 0.48) to yield the imide **3a** as a white powder (0.0325 g, 0.0843 mmol) in 43% yield. Two inseparable isomers: ^{1}H NMR (500 MHz, $CDCl_3$) δ 7.80-7.78 (m, 4H), 7.74-7.71 (m, 4H), 7.45 (dd, J = 6.1, 3.2 Hz, 2H), 7.42-7.39 (m, 4H), 7.31 (dd, J = 5.4, 3.4 Hz, 2H), 7.19 (dd, J = 5.6, 3.2 Hz, 2H), 7.14 (dd, J = 5.4, 2.9 Hz, 2H), 4.91-4.88 (m, 4H), 3.27-3.25 (m, 4H), 3.13 (t, J = 7.1 Hz, 2H), 3.02 (t, J = 6.8 Hz, 2H), 0.84-0.79 (m, 4H), 0.71 (t, J = 6.6 Hz 3H), 0.42-0.34 (m, 4H), 0.11 (t, J = 6.8 Hz, 3H). ^{13}C NMR (125 MHz, $CDCl_3$) δ 176.7, 176.6, 141.1, 138.7, 138.2, 135.8, 132.4, 132.2, 127.49, 127.47, 127.0, 126.8, 125.9, 125.8, 125.0, 124.2, 123.4, 122.4, 46.8, 46.6, 45.4 (2), 38.4, 38.3, 29.2, 29.1, 19.7, 19.4, 13.6, 12.8. IR (cm^{-1}) 1695, 1460, 1435, 1398, 1341, 1292, 1192, 1132, 935, 897, 849, 754, 721.

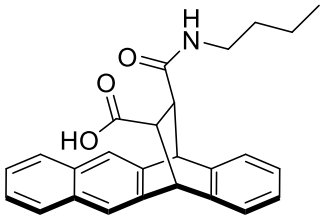

***N*-butyl-5,12-dihydronapthacene-5,12-endo-α,β-succinamic acid (3b):** 5,12-Dihydro-5,12-ethano-napthacene-13,14-dicarboxylic acid anhydride (0.0565 g, 0.173 mmol) was dissolved in CH_2Cl_2 (2 mL) and cooled to 0 °C. To the resulting suspension, *N*-butylamine (0.03 mL, 0.3 mmol) in CH_2Cl_2 (0.1 mL) was added dropwise. The mixture was then stirred at 0 °C for 3 h and then brought to room temperature. The pH of the solution was adjusted to 10 with 1 M NaOH and extracted with water (×3). The pH of the combined aqueous layers was adjusted to 4 with 1 M HCl, which resulted in a white precipitate that was vacuum filtered. The crude product was

triturated with toluene, yielding a white powder that was collected via vacuum filtration. This produced the desired product **3b** (0.0164 g, 0.0415 mmol) in 24% yield. ^{1}H NMR (500 MHz, DMSO-d_6) δ 7.85-7.77 (m, 5H), 7.42 (dd, J = 6.1, 3.2 Hz, 2H), 7.32 (d, J = 6.8 Hz, 1H), 7.11 (d, J = 6.4 Hz, 1H), 7.05 (t, J = 6.6 Hz, 1H) 7.00 (t, J = 6.8 Hz, 1H), 4.63 (d, J = 1.5 Hz, 1H), 4.50 (d, J = 2.5 Hz, 1H), 3.22 (dd, J = 10.7, 2.4 Hz, 1H), 2.99-2.83 (m, 3H), 1.37-1.26 (m, 4H), 0.86 (t, J = 7.1 Hz, 3H). ^{13}C NMR (125 MHz, DMSO-d_6) δ 172.5, 169.6, 141.7, 140.84, 140.81, 140.5, 131.51, 131.49, 127.3, 127.2, 125.37, 125.35, 125.33, 125.1, 125.0, 124.4, 121.2, 120.8, 47.9, 47.5, 46.7, 45.1, 38.1, 31.2, 19.5, 13.7. IR (cm^{-1}) 1711, 1670, 1643, 1562, 1437, 1381, 1321, 1256, 1207, 1165, 947, 881, 687, 665.

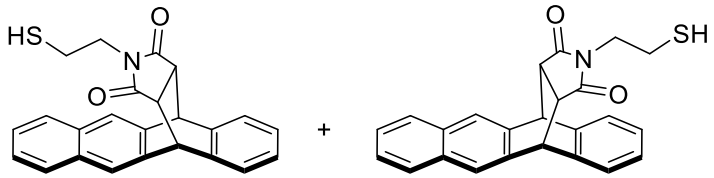

5,12-Dihydro-5,12-ethano-napthacene-15-*N*-(2-sulfanylethyl)pyrrolidine-14,16-dione (4a): Open to the air, 5,12-dihydro-5,12-ethano-napthacene-13,14-dicarboxylic acid anhydride (0.1204 g, 0.3689 mmol), cysteamine (0.0380 g, 0.492 mmol), and acetic acid (5 mL) were added to a round bottom flask. The mixture was then refluxed for 8.5 h and then cooled to room temperature. The mixture was then poured into water (10 mL) to form a white precipitate. The powder was collected via vacuum filtration and rinsed with water three times. The product was dried overnight, which provided 0.1092 g (0.2847 mmol) of **4a** in 77% yield. Major Isomer: ^{1}H NMR (500 MHz, $CDCl_3$) δ 7.81-7.78 (m, 4H), 7.46 (dd, J = 6.1, 3.2 Hz, 2H), 7.32 (dd, J = 5.4, 3.4 Hz, 2H), 7.17 (dd, J = 5.4, 2.9 Hz, 2H), 4.91 (s, 2H), 3.34-3.28 (m, 4H), 1.88 (q, J = 7.8 Hz, 2H), 1.04 (t, J = 9.3 Hz, 1H). ^{13}C NMR (125 MHz, $CDCl_3$) δ 176.2, 138.3, 132.2, 127.2, 126.0, 125.0, 124.2, 122.5, 46.6, 45.4, 41.4, 20.8. Minor Isomer: ^{1}H NMR (500 MHz, $CDCl_3$) δ 7.74 (dd, J = 5.9, 3.4 Hz, 2H), 7.72 (s, 2H), 7.44-7.41 (m, 4H), 7.20 (dd, J = 5.4, 2.9 Hz, 2H), 4.90 (s, 2H), 3.34-3.28 (m, 2H), 3.19 (t, J = 7.6 Hz, 2H), 1.64-1.58 (m, 2H), 0.68 (t, J = 8.5 Hz, 1H). ^{13}C NMR (125 MHz, $CDCl_3$) δ 176.3, 140.9, 138.2, 135.7, 132.2, 127.4, 126.9, 126.1, 123.4, 46.8, 45.4, 41.2, 20.5. IR (mixture, cm^{-1}) 1771, 1695, 1437, 1395, 1337, 1260, 1155, 893, 847, 764.

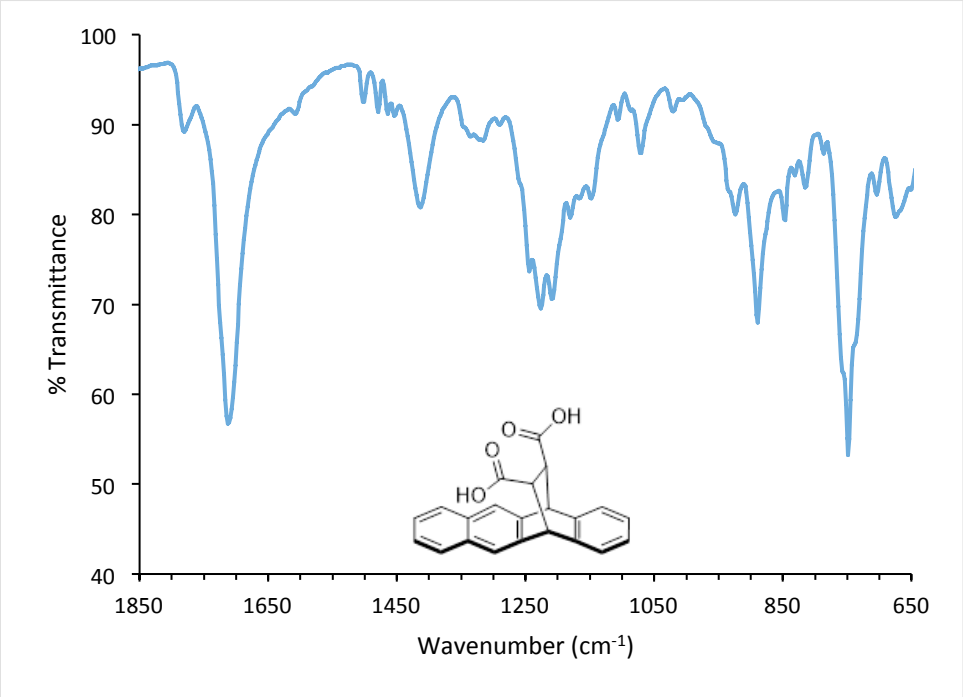

Figure S1: ATR-IR spectra of 5,12-dihydro-5,12-ethano-napthacene-13,14-dicarboxylic acid (**2**).

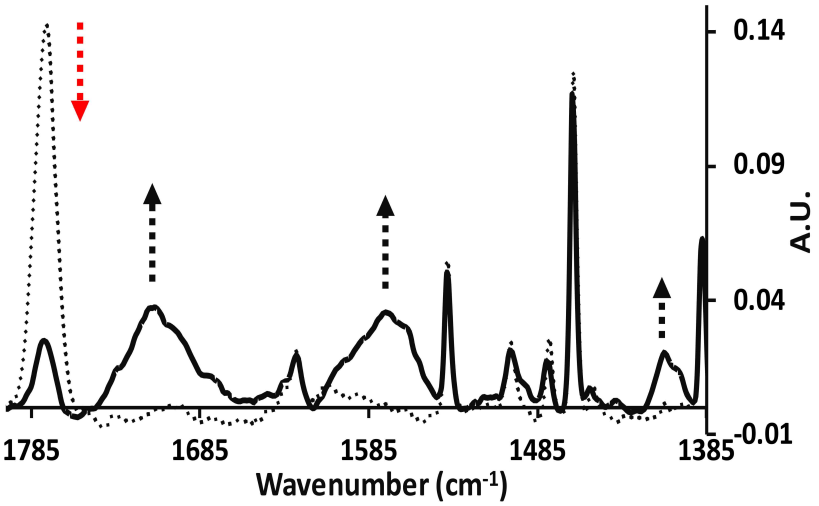

Figure S2: PM-IRRAS spectra of hydrolysis reaction of **1** (dotted line) to form the diacid **2** (solid line). A broad stretch at 1561 cm^{-1}, along with a carbonyl stretch at 1698 cm^{-1}, suggests the presence of more extensive hydrogen bonding in this sample. We attribute this feature to hydrogen bonding in the reacted films as typical diagnostic features, such as a shift in carbonyl frequencies along with the observation of stretch broadening,[6–8] are present. Typically, this occurs via one of two scenarios: in the first, the diacid bonds with excess water present, in the second, hydrogen bonding occurs intramolecularly. In order to investigate the former, the samples were exposed to vacuum (~5×10^{-6} Torr) for 2 h. A decrease in the stretch at 1561 cm^{-1} was not observed. The same is true for films placed in a desiccator containing P_2O_5 for several days. Thus, we believe the most likely explanation for this phenomenon is intramolecular hydrogen bonding, which is common for maleic acid and other analogues.[8–11]

XPS Analysis of Cysteamine secondary reaction

Complimentary assessment with X-ray photoelectron spectroscopy (XPS), which is particularly effective at elemental and chemical analysis, provides a fuller picture of the formed products. Deconvolution of the O 1s and N 1s signals can provide an idea of the relative amounts of imide to acid amide. Within the O 1s signal (Figure S3a) are two peaks. The first, at 532.1 eV, has been attributed to a carbonyl oxygen while the second at 531.1 eV is assigned to a carboxylate which is commonly found at ~1 eV lower binding energy than the uncharged oxygen.[12] Signal integration of these two components indicate that 22% of the surface oxygen is from a carboxylate while the remainder is a carbonyl. In a similar manner, deconvolution of the N 1s region yielded two peaks (Figure S3b). The first, with a binding energy of 399.8 eV is typical of uncharged amide and imide nitrogens.[13] The second peak at 401.3 eV, has been attributed to a charged amide from proton transfer and/or hydrogen bonding.[13,14] Signal integration of the two peaks yielded a ratio of 1.4:1, indicating that 41% of the surface species are charged. Taken together the N 1s and O 1s signals are suggestive of hydrogen boding between the carboxylic acid and amide. Here it is assumed that nearly all the acid-amide is hydrogen bonding, based on similar analogues,[15] and as such this indicates that roughly 40% is acid amide, while the remaining 60% is imide. Using this information, the sulfur to oxygen ratio (1 to 2.3) can be used to estimate the amount of cysteamine that has bonded to each maleic anhydride. If 60% of the surface is imide **4a** (1 S: 2 O) and 40% of the surface is acid amide **4b** (1 S: 3 O) the expected ratio of signals is 1 to 2.4, almost identical to the measured amount. Any disulfide present is less than 10% of the species.

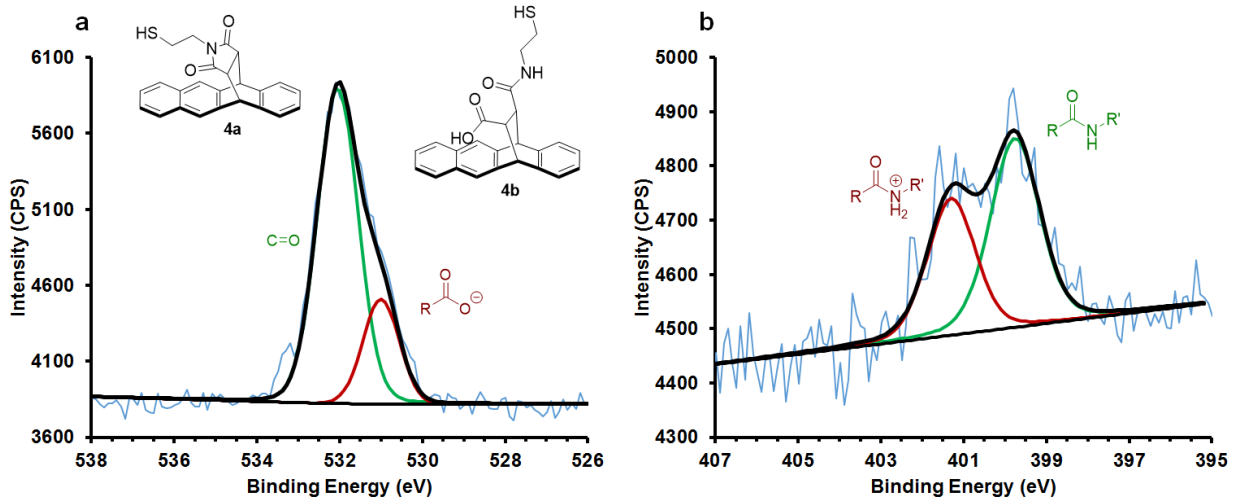

Figure S3: Deconvoluted XPS spectra of the (a) O 1s and (b) N 1s region for a cysteamine reacted thin-film. The green peaks are attributed to the neutral species while the peaks in red are assigned to charged/hydrogen bonded species. All peaks are reference to the C 1s signal at 284.6 eV. Discussion of these signals is above.

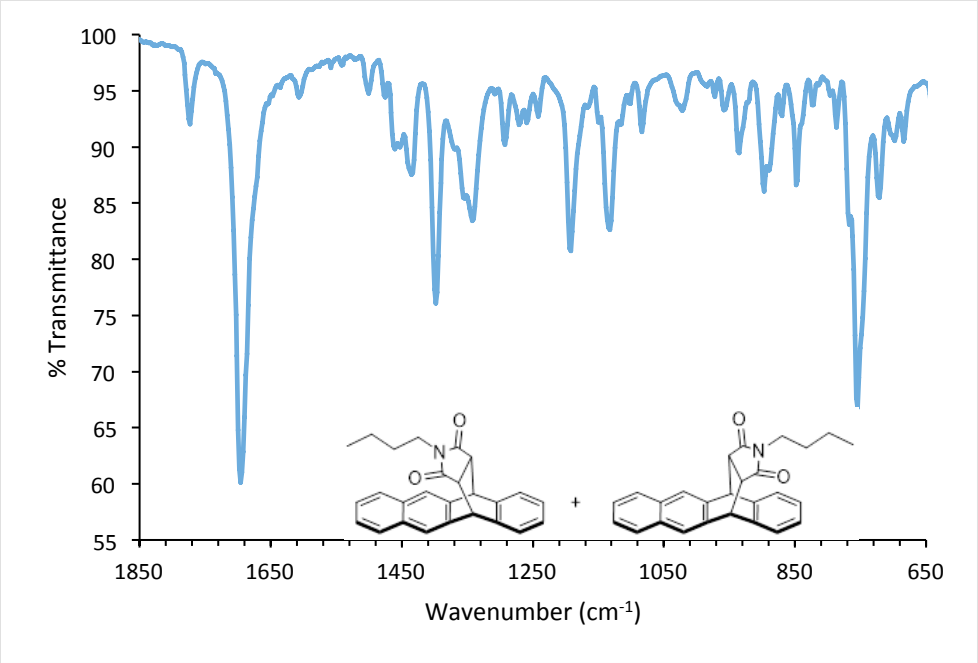

Figure S4: ATR-IR spectra of **3a**.

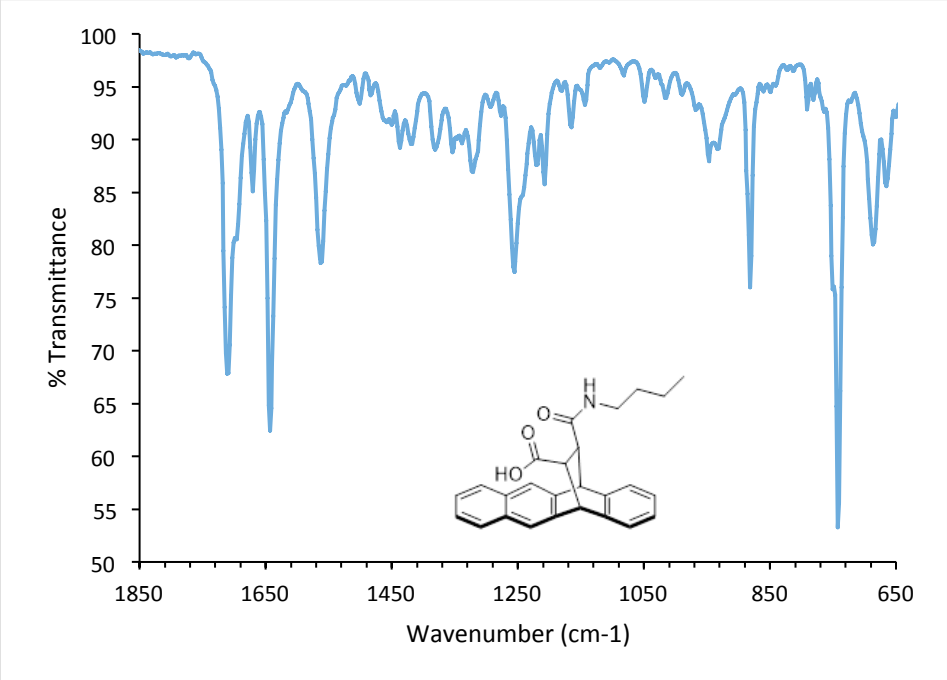

Figure S5: ATR-IR spectra of **3b**.

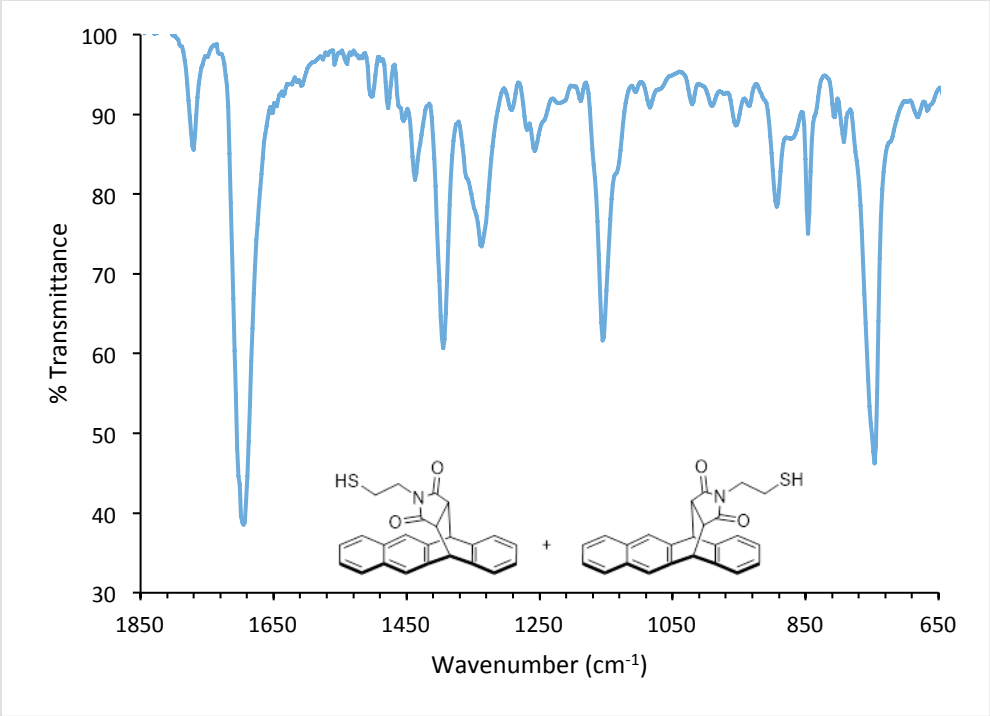

Figure S6: ATR-IR spectra of **4a**.

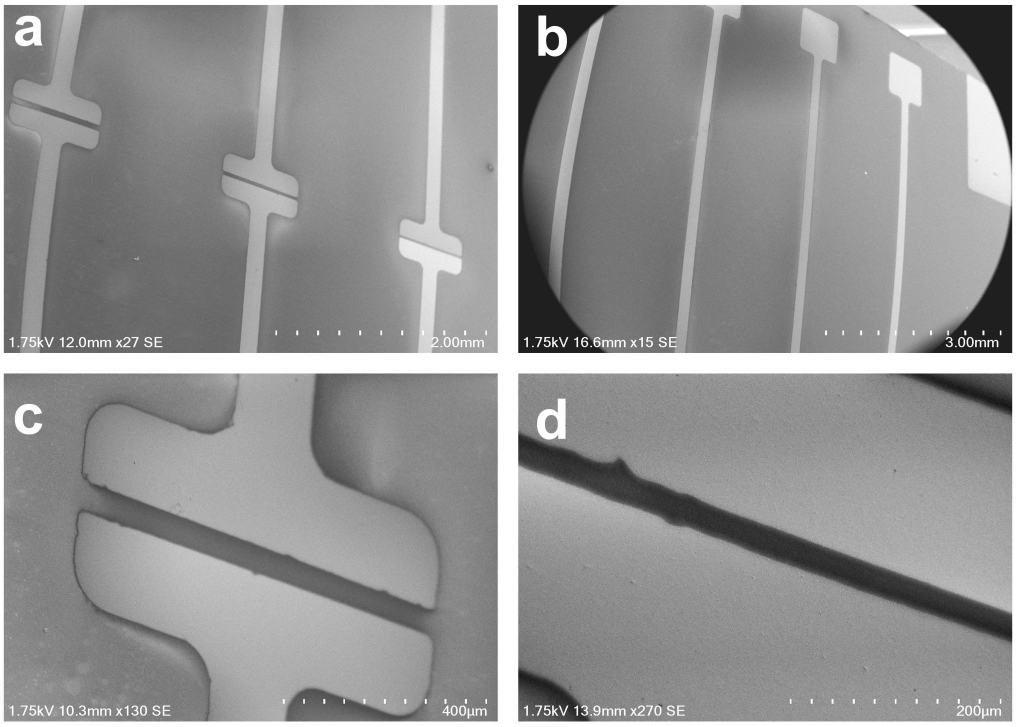

Figure S7: (a-d) Additional SEM images of Ag electrodes deposited onto unreacted tetracene (150 nm) on a gold coated PET substrate. All SEM image are *before* bending and were imaged at an aceleration voltage of 1.75 kV and titled 70°.

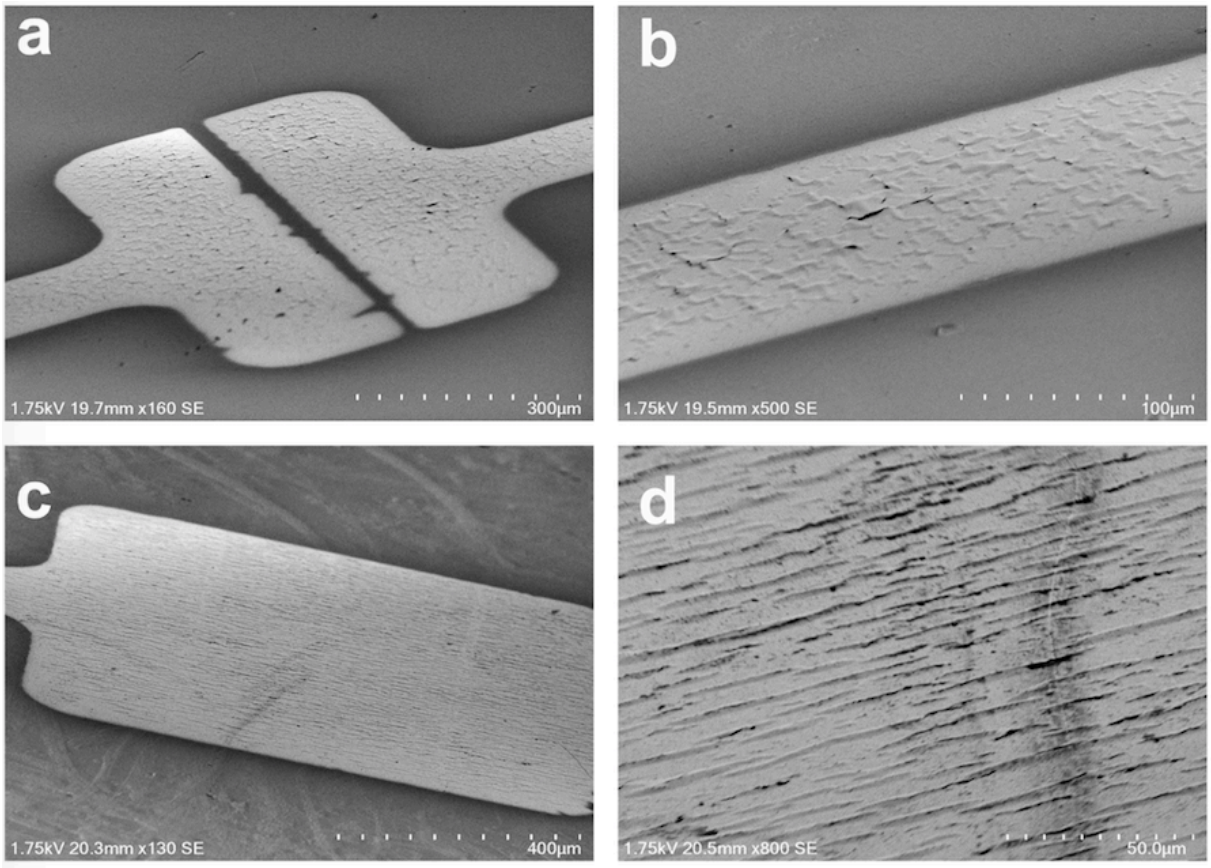

Figure S8: (a-d) Additional SEM images of Ag electrodes deposited onto unreacted tetracene (150 nm) on a gold coated PET substrate. All SEM image are *after* 50 bending cycles and were imaged at an aceleration voltage of 1.75 kV and titled 70°.

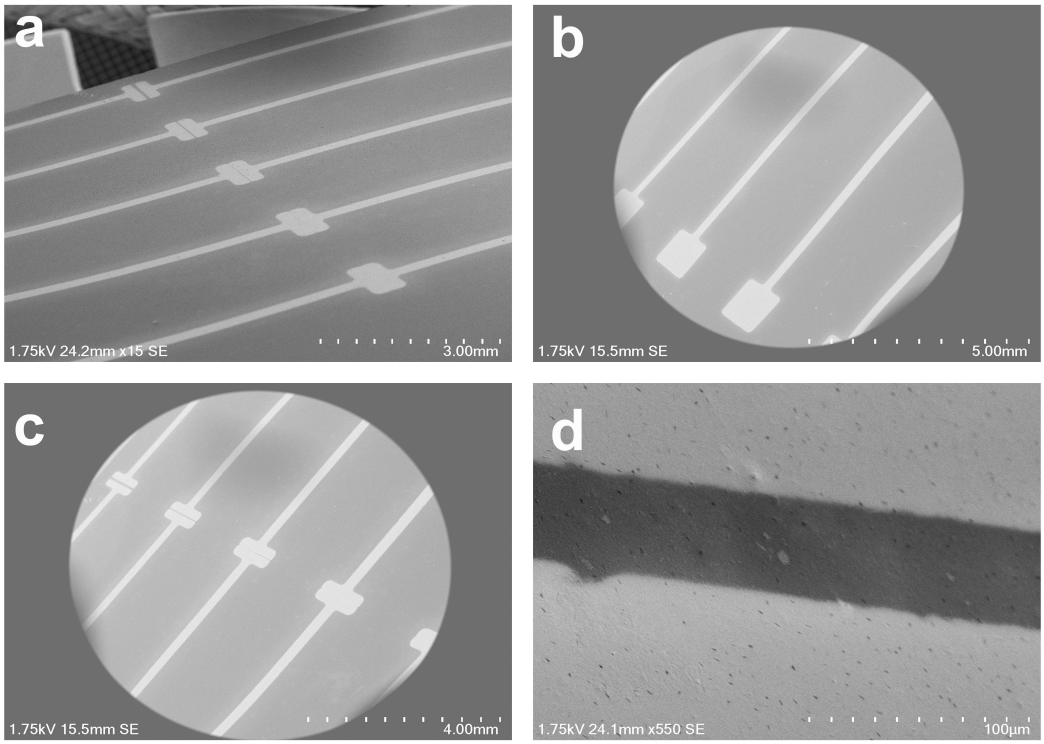

Figure S9: (a-d) Additional SEM images of Ag electrodes deposited onto reacted tetracene (150 nm) on a gold coated PET substrate. The reaction consists of, first, maleic anhydride precursor formation followed by cysteamine reaction. All SEM image are *before* bending and were imaged at an aceleration voltage of 1.75 kV and titled 70°.

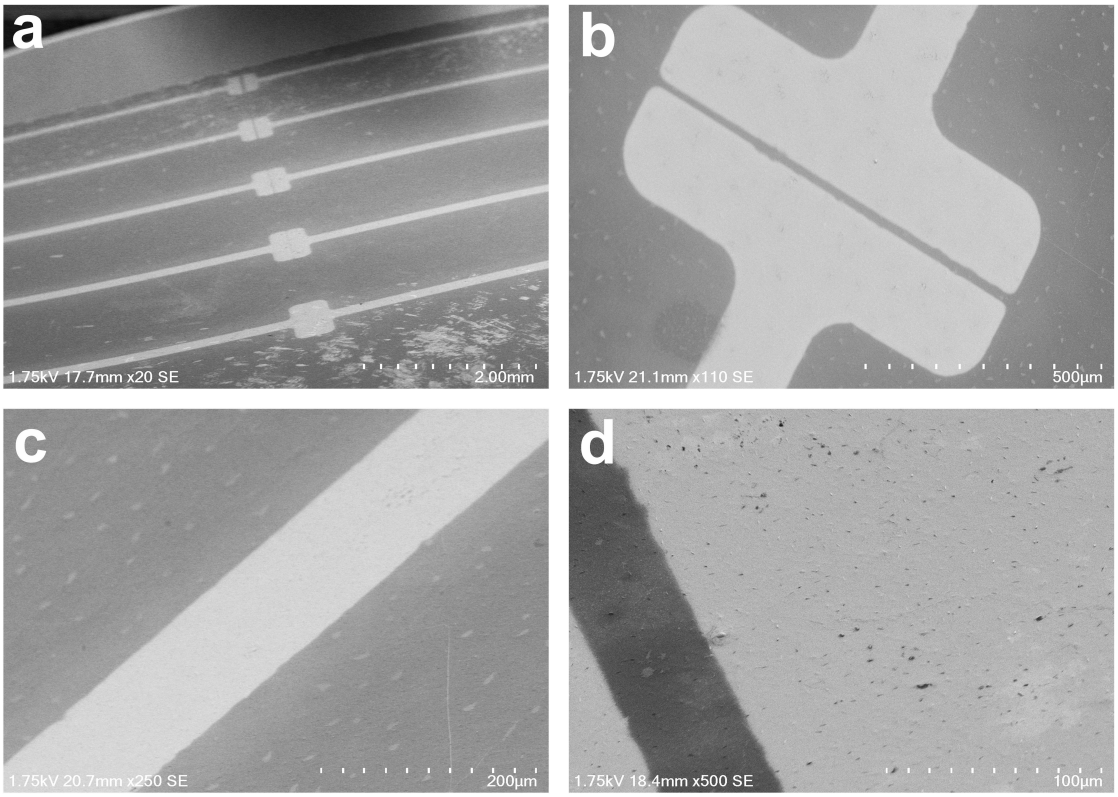

Figure S10: (a-d) Additional SEM images of Ag electrodes deposited onto reacted tetracene (150 nm) on a gold coated PET substrate. The reaction consists of, first, maleic anhydride precursor formation followed by cysteamine reaction. All SEM image are *after* 100 bending cycles and were imaged at an aceleration voltage of 1.75 kV and titled 70°. White areas visible on the side of (a) are due to handling damage during the bending test.

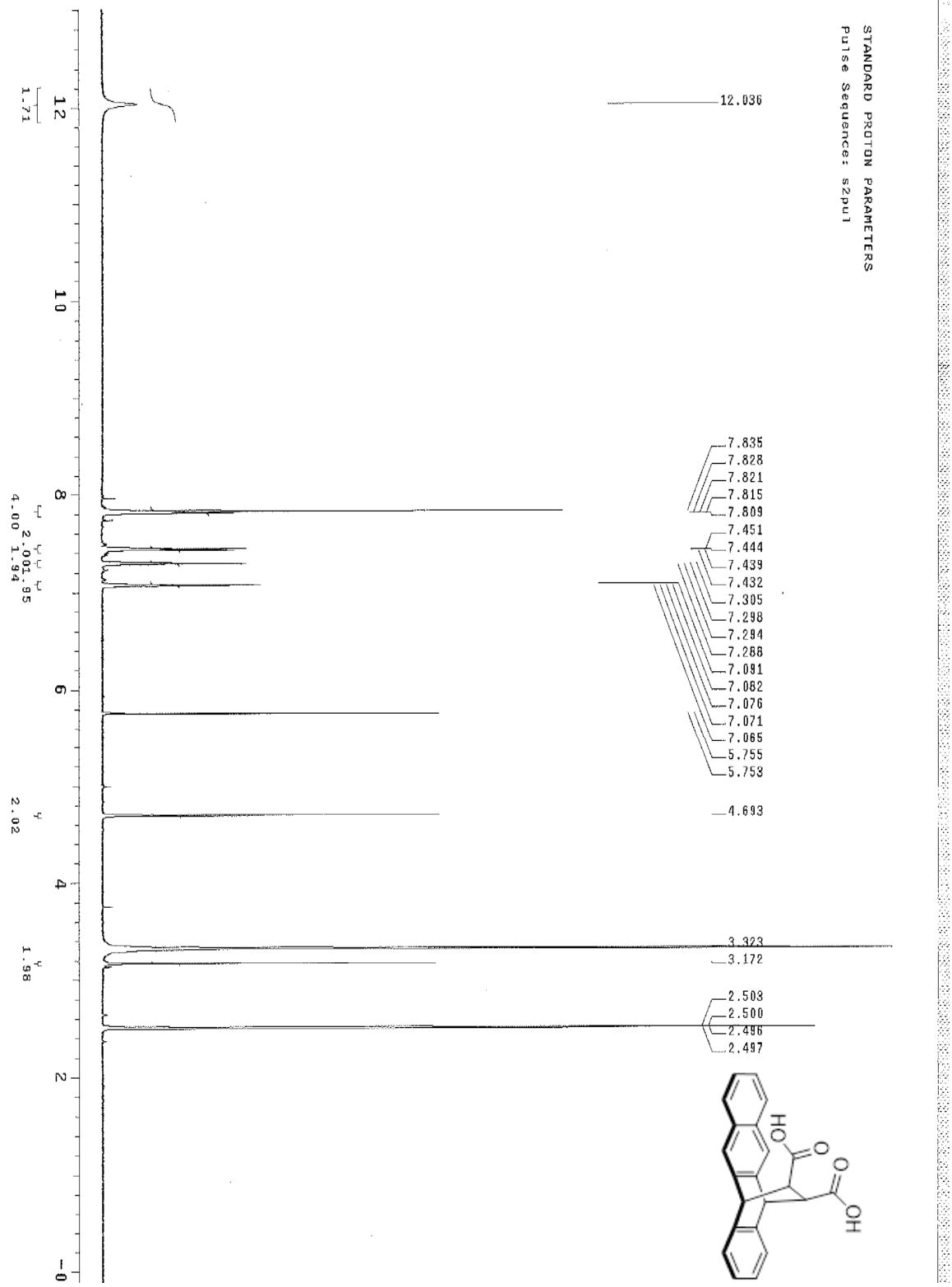
STANDARD PROTON PARAMETERS
Pulse Sequence: s2pul
12.036
7.835
7.828
7.821
7.815
7.809
7.451
7.444
7.439
7.432
7.305
7.298
7.294
7.288
7.081
7.062
7.076
7.071
7.065
5.755
5.753
4.693
3.323
3.172
2.503
2.500
2.496
2.497
HO
O
O
OH
1.71
4.00
2.00
1.94
2.02
1.98
12
10
8
6
4
2
0

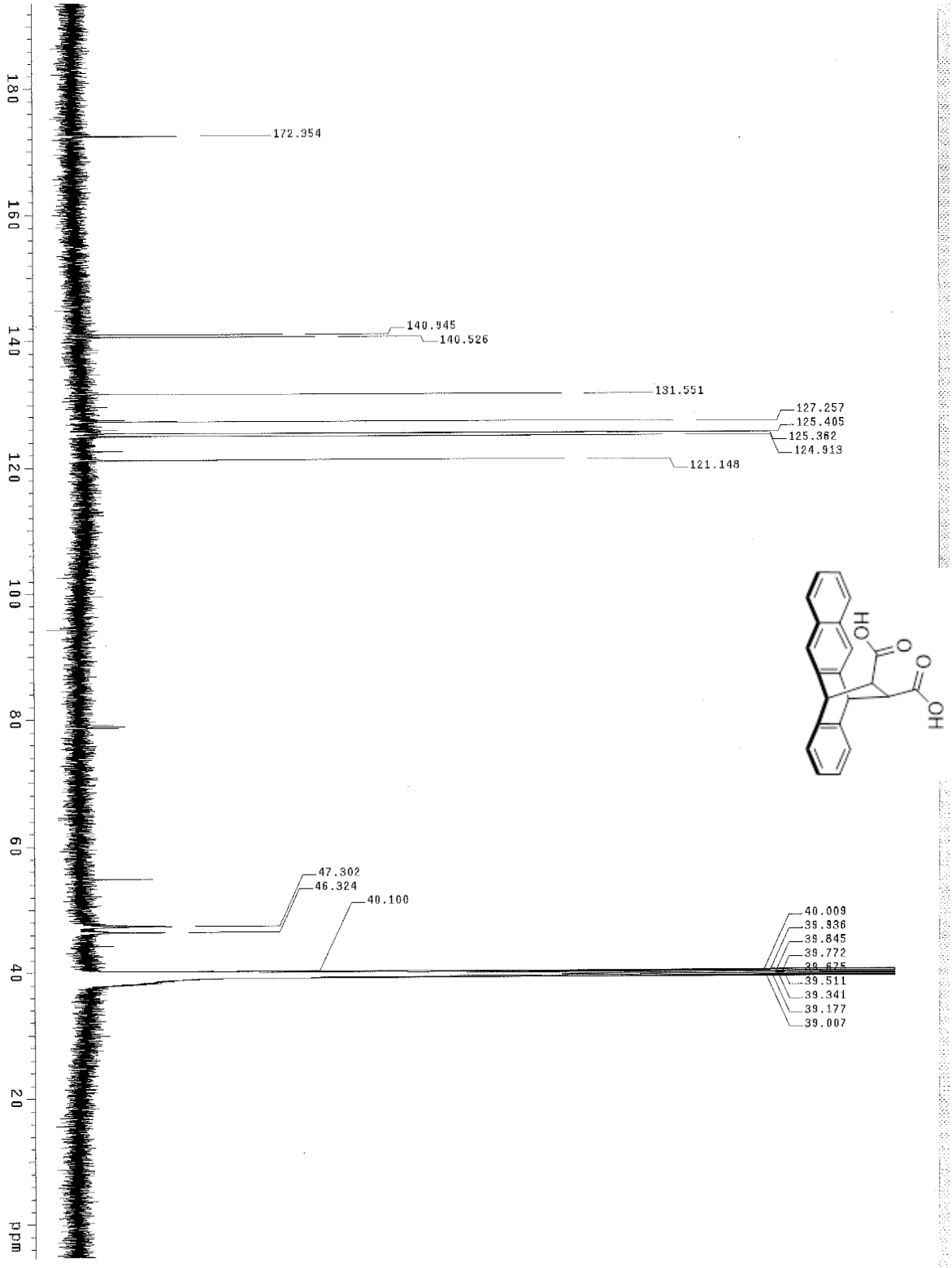
180
160
140
120
100
80
60
40
20
ppm
172.354
140.945
140.526
131.551
127.257
125.405
125.362
124.913
121.148
47.302
46.324
40.100
40.009
39.936
39.845
39.772
39.675
39.511
39.341
39.177
39.007
HO
O
O
OH

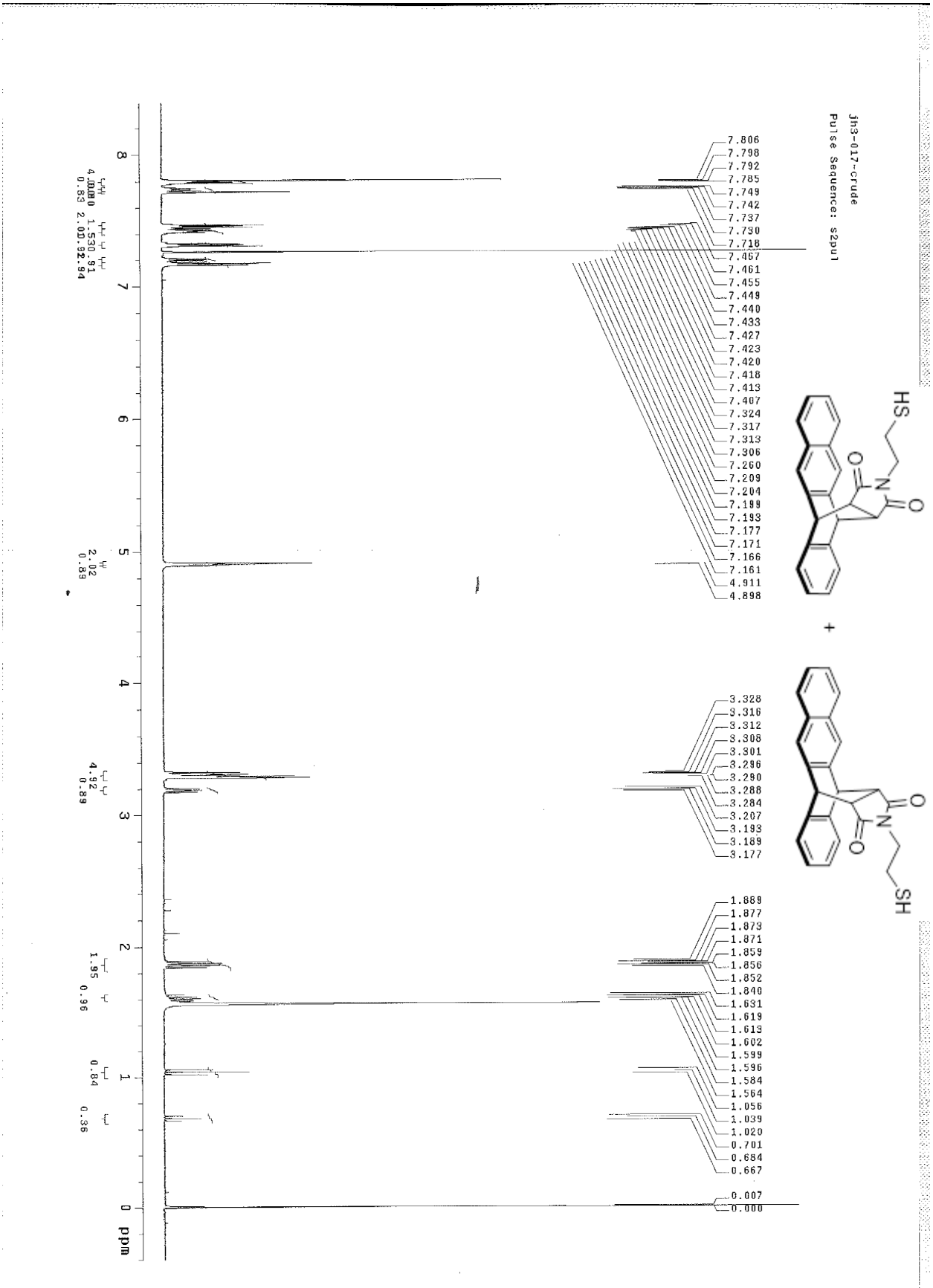
jh3-017-crude
Pulse Sequence: s2pul
7.806
7.798
7.792
7.785
7.749
7.742
7.737
7.730
7.718
7.467
7.461
7.455
7.449
7.440
7.433
7.427
7.423
7.420
7.418
7.413
7.407
7.324
7.317
7.313
7.306
7.260
7.209
7.204
7.199
7.193
7.177
7.171
7.166
7.161
4.911
4.898
3.328
3.316
3.312
3.308
3.301
3.296
3.290
3.288
3.284
3.207
3.193
3.189
3.177
1.889
1.877
1.873
1.871
1.859
1.856
1.852
1.840
1.631
1.619
1.613
1.602
1.599
1.596
1.584
1.564
1.056
1.039
1.020
0.701
0.684
0.667
0.007
0.000
HS
SH
+
ppm

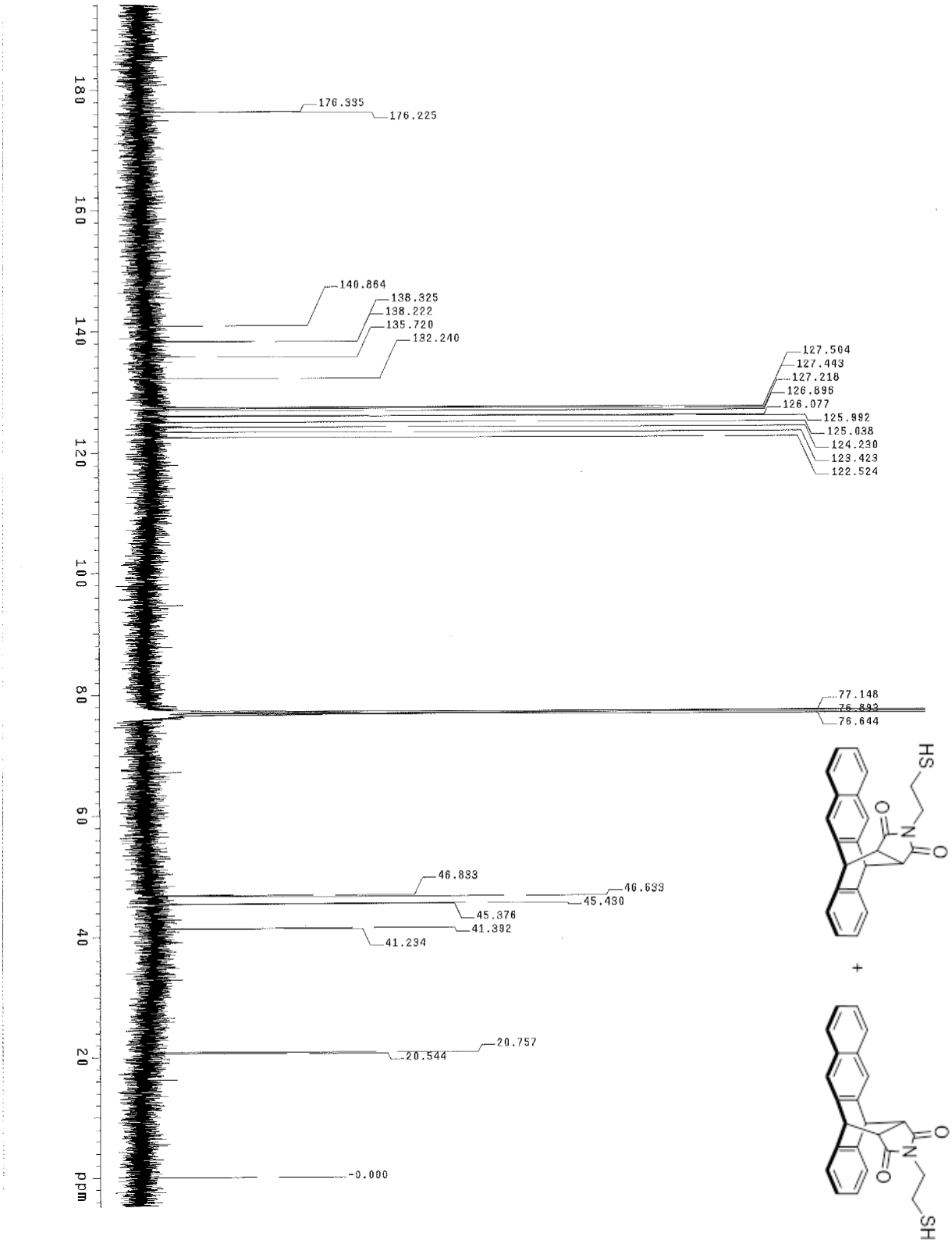
176.335
176.225
140.864
138.325
138.222
135.720
132.240
127.504
127.443
127.218
126.896
126.077
125.992
125.038
124.230
123.423
122.524
77.148
76.893
76.644
46.883
46.633
45.430
45.376
41.392
41.234
20.757
20.544
-0.000
ppm
180
160
140
120
100
80
60
40
20
HS
O
N
O
+
O
N
O
SH

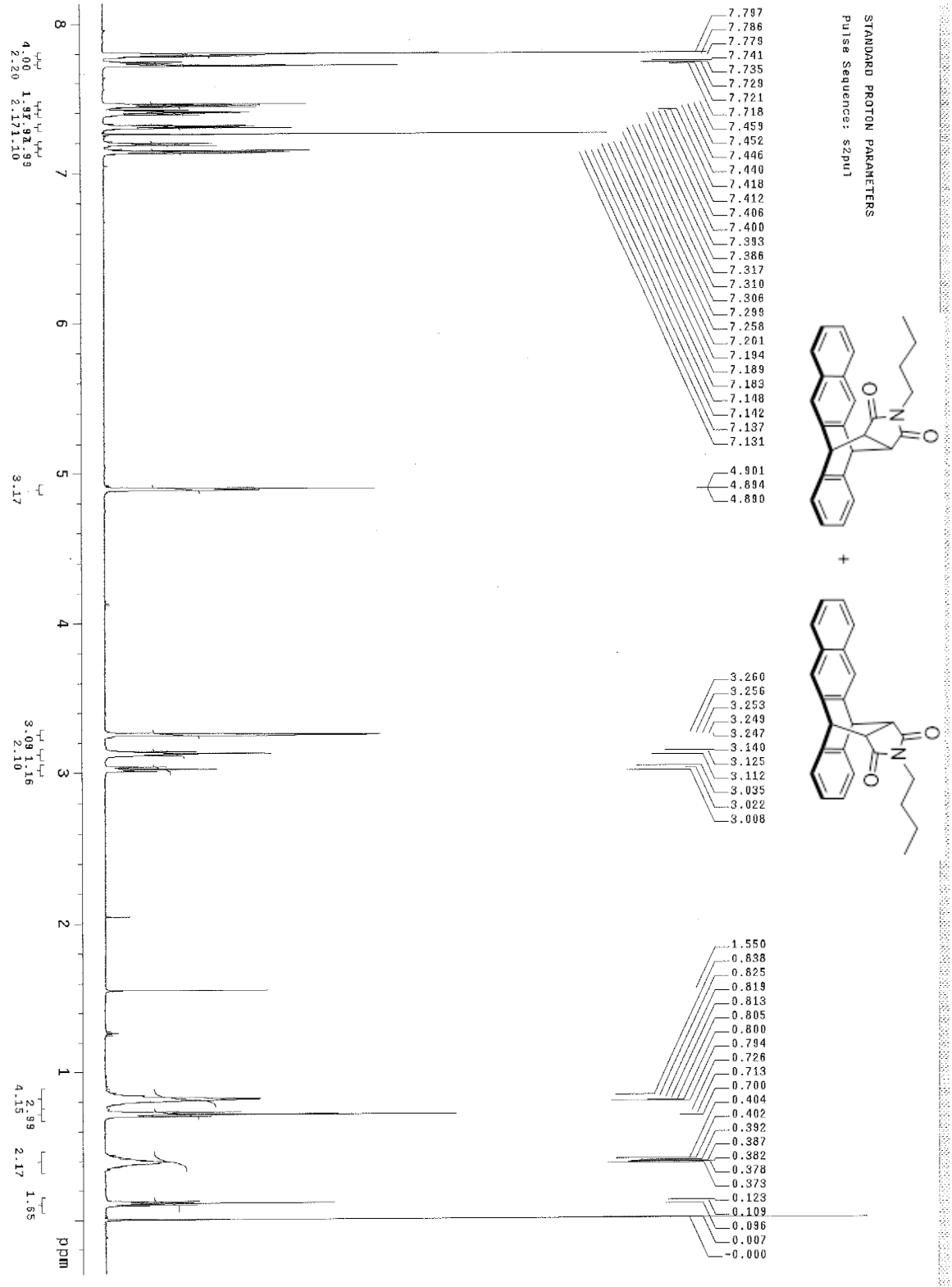
STANDARD PROTON PARAMETERS
Pulse Sequence: s2pul
7.797
7.786
7.779
7.741
7.735
7.729
7.721
7.718
7.459
7.452
7.446
7.440
7.418
7.412
7.406
7.400
7.393
7.386
7.317
7.310
7.306
7.299
7.258
7.201
7.194
7.189
7.183
7.148
7.142
7.137
7.131
4.901
4.894
4.890
3.260
3.256
3.253
3.249
3.247
3.140
3.125
3.112
3.035
3.022
3.008
1.550
0.838
0.825
0.819
0.813
0.805
0.800
0.794
0.726
0.713
0.700
0.404
0.402
0.392
0.387
0.382
0.378
0.373
0.123
0.109
0.096
0.007
-0.000
4.00
2.20
1.97
2.17
1.99
2.10
3.17
3.09
1.16
2.10
2.99
4.15
2.17
1.65
+
ppm

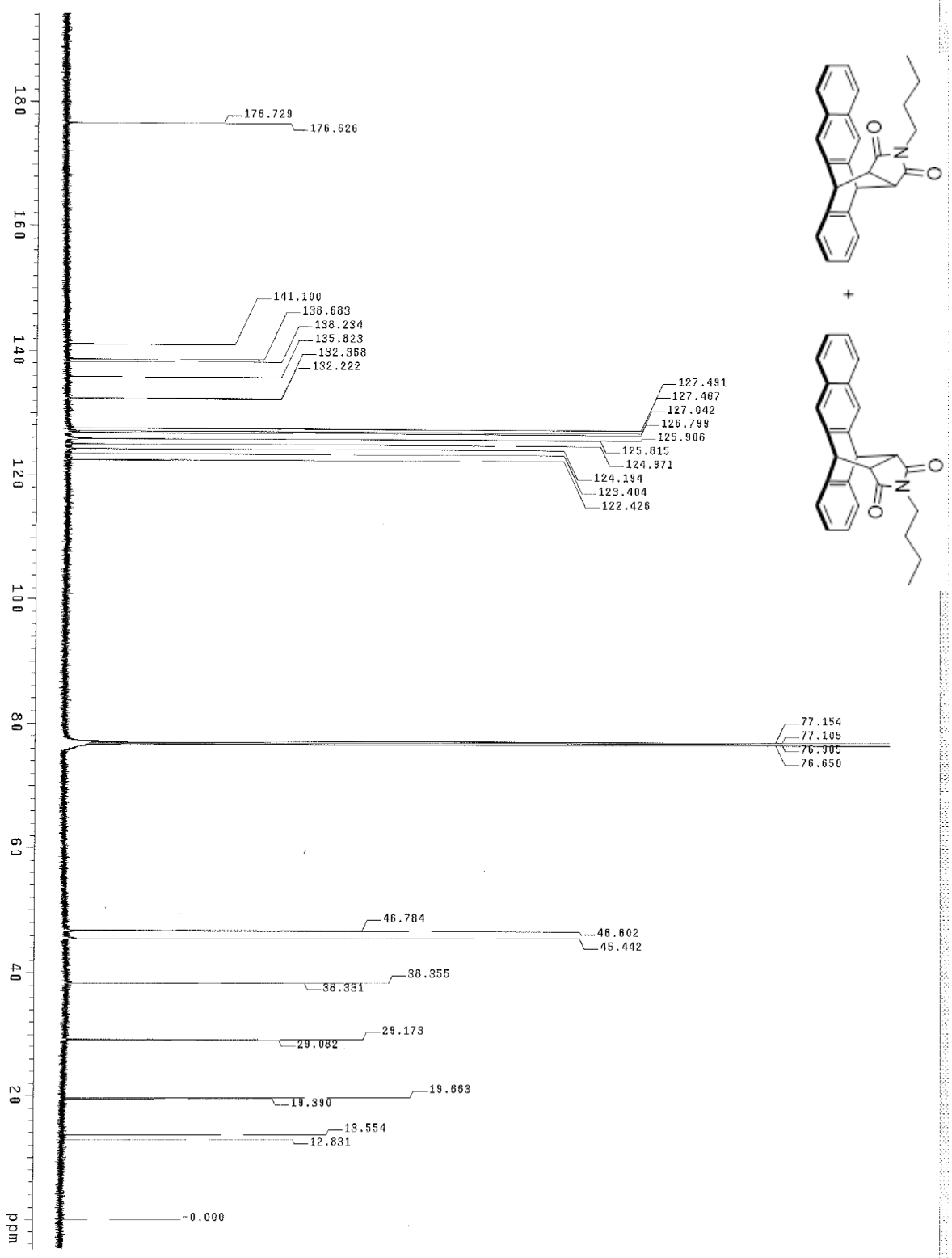
176.729
176.626
141.100
138.683
138.234
135.823
132.368
132.222
127.491
127.467
127.042
126.798
125.906
125.815
124.971
124.194
123.404
122.426
77.154
77.105
76.905
76.650
46.784
46.602
45.442
38.355
38.331
29.173
29.082
19.863
19.390
13.554
12.831
0.000
ppm

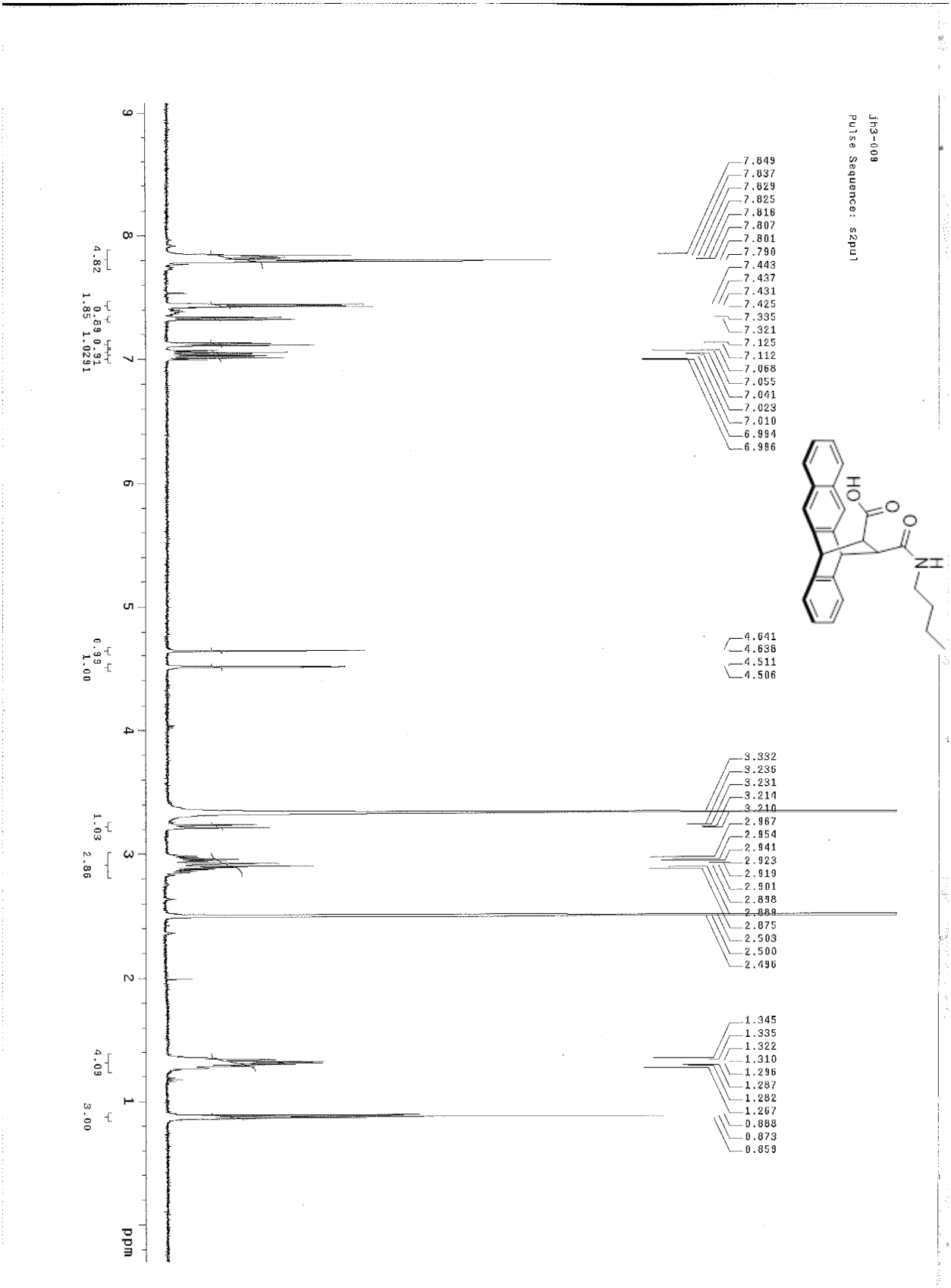
jh3-009
Pulse Sequence: s2pul
7.849
7.837
7.829
7.825
7.816
7.807
7.801
7.790
7.443
7.437
7.431
7.425
7.335
7.321
7.125
7.112
7.068
7.055
7.041
7.023
7.010
6.994
6.986
4.641
4.638
4.511
4.506
3.332
3.236
3.231
3.214
3.210
2.967
2.954
2.941
2.923
2.919
2.901
2.898
2.889
2.875
2.503
2.500
2.496
1.345
1.335
1.322
1.310
1.296
1.287
1.282
1.267
0.888
0.873
0.859
4.82
0.89
0.91
1.85
1.0291
0.89
1.00
1.03
2.86
4.09
3.00
HO
O
O
N
H
ppm

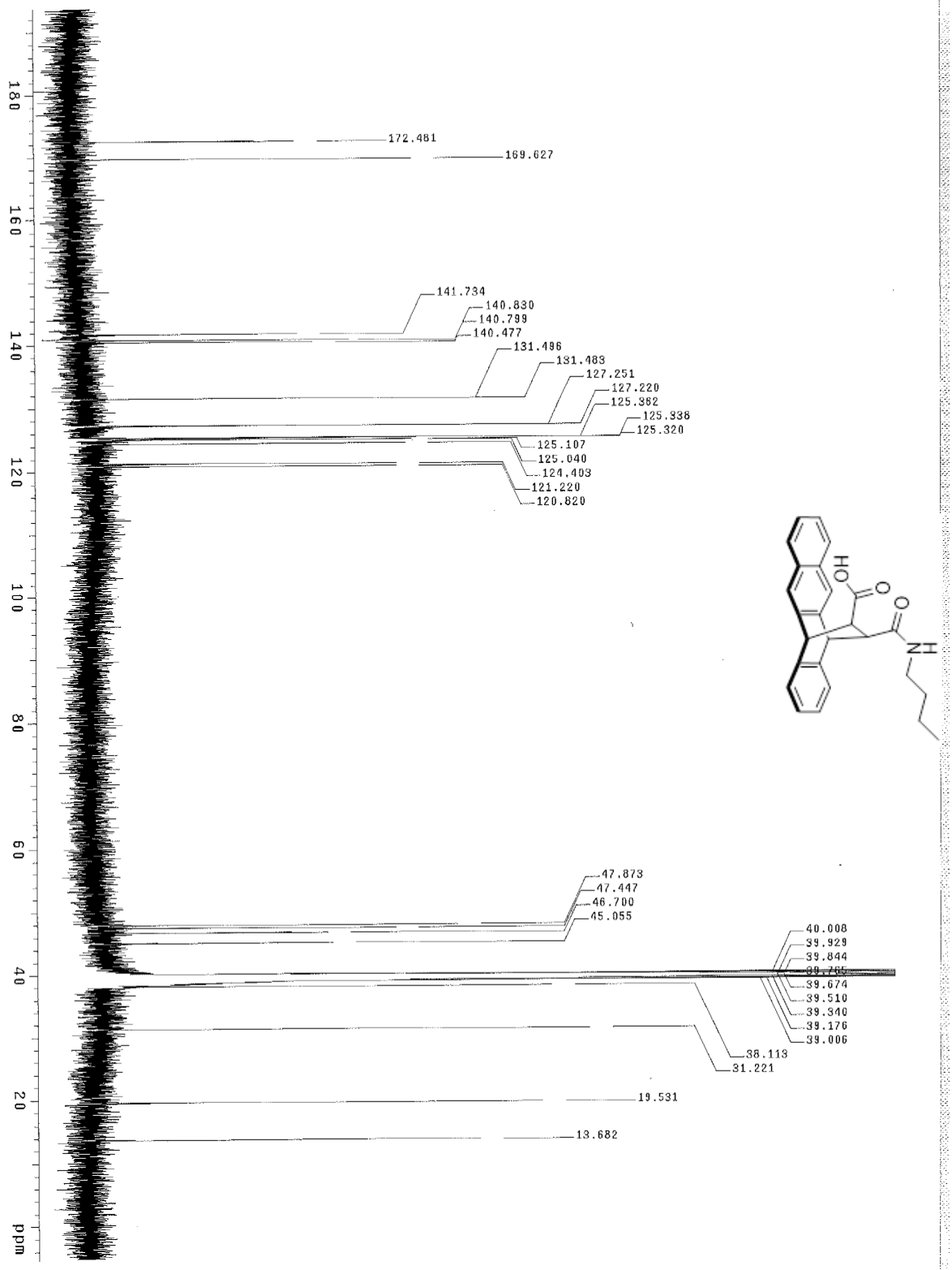
172.481
169.627
141.734
140.830
140.799
140.477
131.496
131.483
127.251
127.220
125.382
125.338
125.320
125.107
125.040
124.403
121.220
120.820
47.873
47.447
46.700
45.055
40.008
39.929
39.844
39.674
39.510
39.340
39.176
39.006
38.113
31.221
19.531
13.682
ppm

XPS Survey Scan

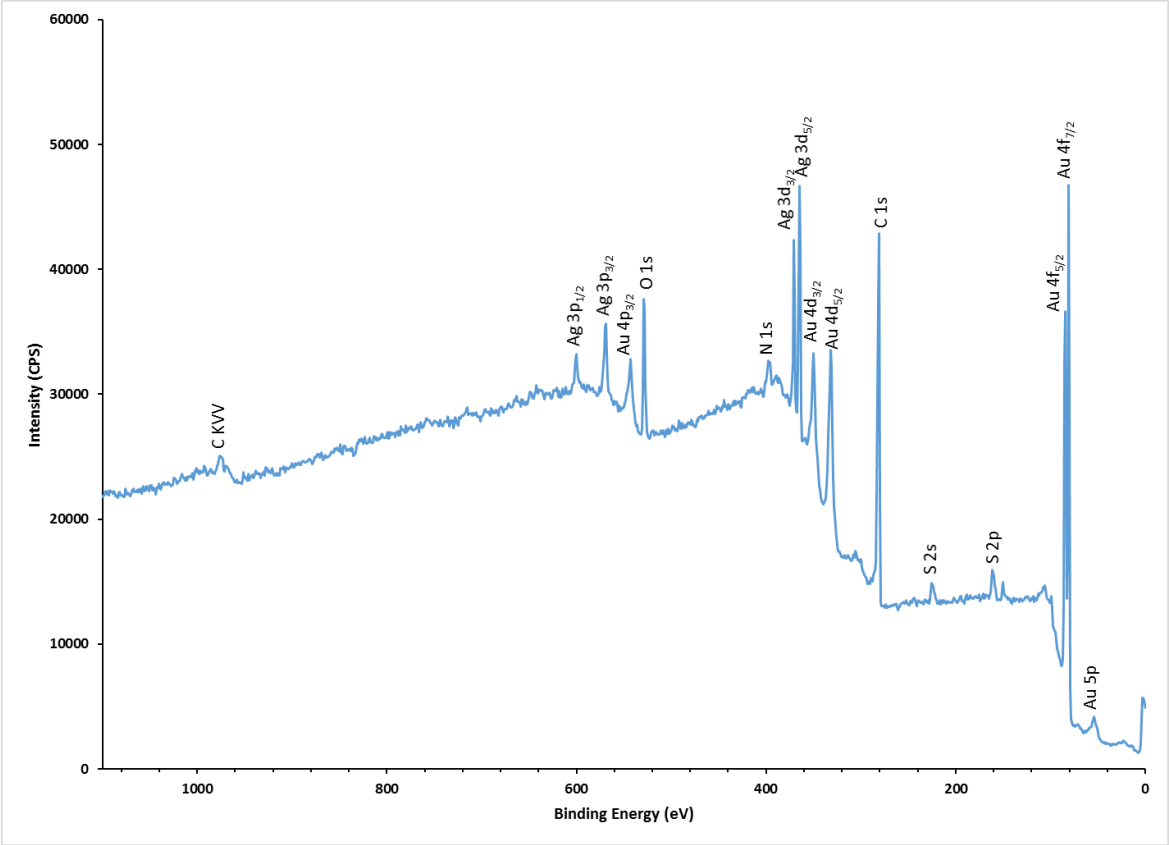

XPS of C 1s Region

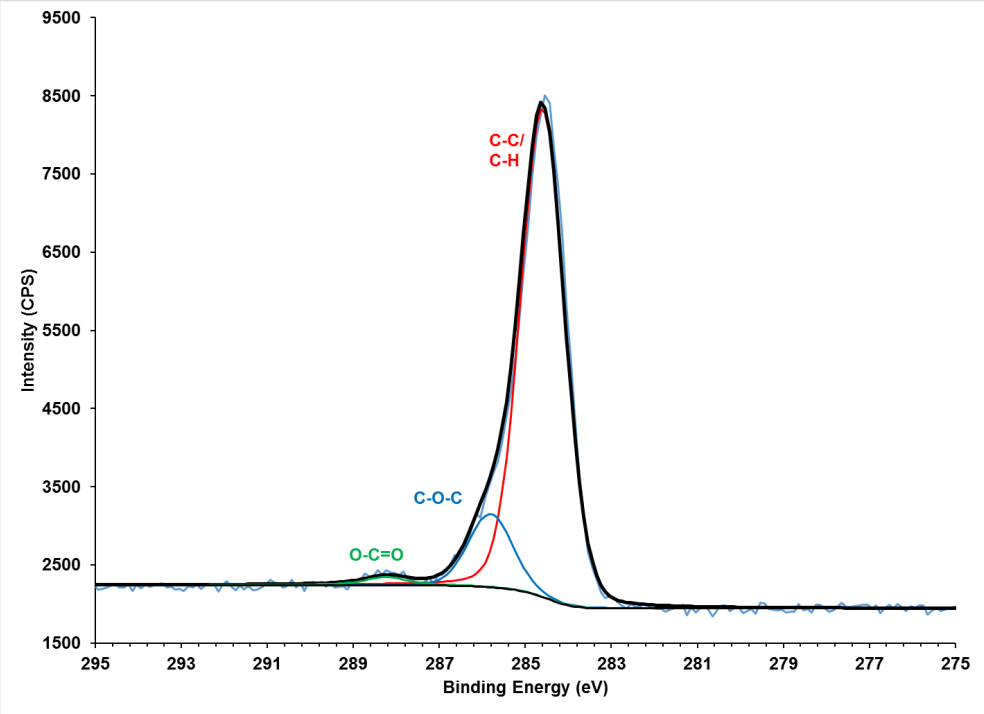

XPS of S 2p Region

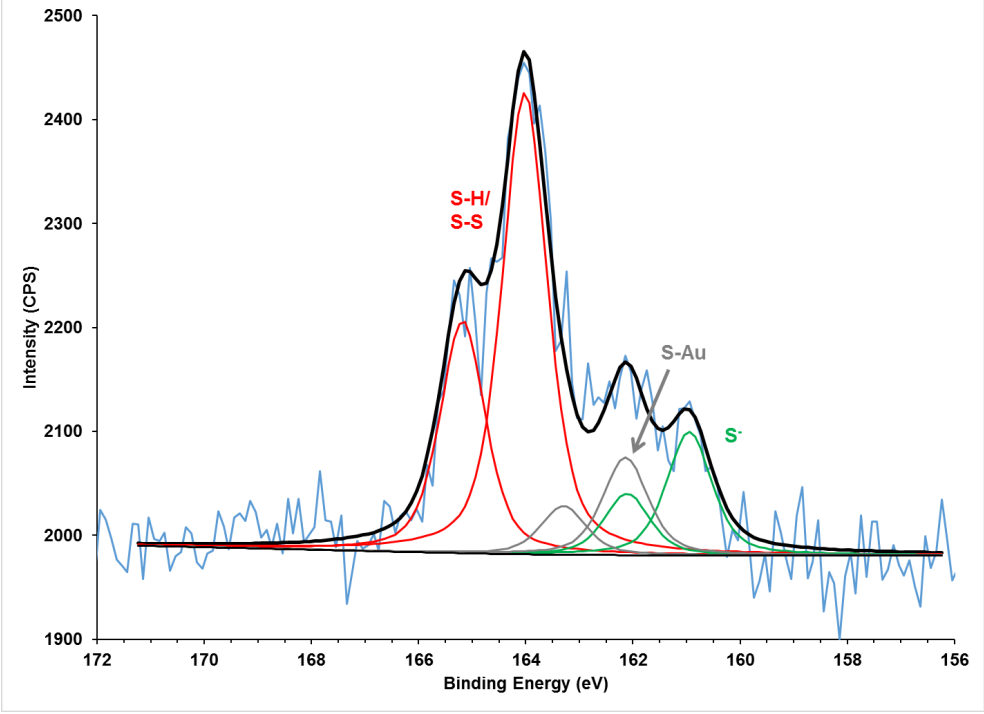

References

1 S. Piranej, D. A. Turner, S. M. Dalke, H. Park, B. A. Qualizza, J. Vicente, J. Chen and J. W. Ciszek, *CrystEngComm*, 2016, **18**, 6062–6068.
2 J.-C. Dupin, D. Gonbeau, P. Vinatier and A. Levasseur, *Phys. Chem. Chem. Phys.*, 2000, **2**, 1319–1324.
3 J. Lee, T. Han, M. Park, D. Y. Jung, J. Seo, H. Seo, H. Cho, E. Kim, J. Chung, S. Chuoi, T. Kim, T. Lee, S. Yoo, *Nat. Commun.*, 2016, **7**, 11791.
4 G. R. Fulmer, A. J. M. Miller, N. H. Sherden, H. E. Gottlieb, A. Nudelman, B. M. Stoltz, J. E. Bercaw and K. I. Goldberg, *Organometallics*, 2010, **29**, 2176–2179.
5 B. A. Qualizza, S. Prasad, M. P. Chiarelli and J. W. Ciszek, *Chem. Commun.*, 2013, **49**, 4495–4497.
6 J. Emsley, *Chem. Soc. Rev.*, 1980, **9**, 91–124.
7 T. Zeergers-Huyskens and L. Sobczyk, *J. Mol. Liq.*, 1990, **46**, 263–284.
8 S. Kawaguchi, T. Kitano and K. Ito, *Macromolecules*, 1991, **24**, 6030–6036.
9 L. Eberson, *Acta Chem. Scand.*, 1959, **13**, 224–235.
10 M. Ilczyszyn, D. Godzisz and M. M. Ilczyszyn, *Spectrochim. Acta. A. Mol. Biomol. Spectrosc.*, 2003, **59**, 1815–1828.
11 H. M. E. Cardwell, J. D. Dunitz and L. E. Orgel, *J. Chem. Soc.*, 1953, **0**, 3740–3742.
12 S. Stepanow, T. Strunskus, M. Lingenfelder, A. Dmitriev, H. Spillmann, N. Lin, J. V. Barth, C. Wöll and K. Kern, *J. Phys. Chem. B*, 2004, **108**, 19392–19397.
13 R. J. J. Jansen and H. van Bekkum, *Carbon*, 1995, **33**, 1021–1027.
14 J. S. Stevens, S. J. Byard, C. C. Seaton, G. Sadiq, R. J. Davey and S. L. M. Schroeder, *Phys. Chem. Chem. Phys.*, 2013, **16**, 1150–1160.
15 R. Francis, P. Raghavaiah and K. Pius, *Acta Crystallogr. Sect. B Struct. Sci. Cryst. Eng. Mater.*, 2014, **70**, 942–947.